12.5 PASSIVE THERMAL RETRIEVALS OF ICE AND LIQUID WATER PATH, EFFECTIVE SIZE AND OPTICAL DEPTH AND THEIR DEPENDENCE ON PARTICLE AND SIZE DISTRIBUTION SHAPE

David L. Mitchell[1], Robert P. d'Entremont[2] and R. Paul Lawson[3]
1. Desert Research Institute, Reno, Nevada
2. Atmospheric and Environmental Research, Inc., Lexington, Massachusetts
3. SPEC Inc., Boulder, Colorado

1. INTRODUCTION

To date, a major limitation imposed on global climate models (GCMs) is the lack of reliable global statistics of ice water path (IWP) and effective particle size (D_{eff}) with which to evaluate predicted cirrus against. The best hope of providing such statistics is through satellite remote sensing, thereby presenting a need for algorithms that retrieve IWP and D_{eff} using radiances measured from satellites.

Cirrus radiative properties depend on vertical profiles of the size and shape of ice particles and the ice-water content (Yoshida and Asano 2005). The bimodal nature of the ice particle size distribution (SD) may also be a significant factor for terrestrial radiation (Mitchell 2002). To date no ice cloud property retrieval scheme has incorporated existing knowledge of ice particle shape and SD bimodality.

Another long-standing problem has been the inability to accurately retrieve LWP, since the microwave radiometer (MWR) uncertainty for LWP < 100 g m^{-2} is 20-30 g m^{-2} (20% to 100%). For higher LWP, the MWR is sufficient. At the North Slope of Alaska (NSA) site for the Atmospheric Radiation and Measurement (ARM) program, the fraction of liquid or mixed phase clouds having LWP < 100 g m^{-2} is greater than 80%, and this fraction is about 50% at mid-latitudes (Dave Turner, 2005 ARM presentation). Without a reliable means of retrieving LWP in the 5-100 g m^{-2} range, it will be difficult to characterize clouds in the arctic, and hence difficult to characterize the arctic radiation balance. This is of particular concern given that the polar regions are expected to be most affected by global warming.

The proposed methodology provides a means of retrieving D_{eff}, water path (WP) and optical depth for ice and liquid water clouds, where the retrievals can be either satellite based or ground-based. The measured thermal radiances are derived from the 2nd and 3rd moments (area and mass) of the particle size distribution, SD. That is, the radiance a sensor measures depends to varying degrees on the cloud particle geometric cross-section (strong absorption) and the particle mass (weak absorption). Moderate absorption in the window region between 8.3-10.2 μm would generally exhibit both area and mass dependence. These retrievals are thus sensitive to the small-particle mode of the SD in cirrus clouds (D < 100 μm), which retrievals using radar (mass-squared dependence) may not be sensitive to. Measurements of the Forward Scattering Spectrometer Probe (FSSP) and the 2DC probe in mid-latitude cirrus (e.g. Ivanova et al. 2001) show that the peak concentration of the small mode is typically 2-3 orders of magnitude greater than the peak concentration in the large SD mode, making D_{eff} retrievals based on only the large mode approximately 45% larger than D_{eff} from retrievals that model both modes. Hence a radar retrieval of D_{eff} that does not "see" the small mode could seriously overestimate D_{eff}.

Corresponding author address: David L. Mitchell, Desert Research Institute, Reno, NV 89512-1095; e-mail: mitch@dri.edu

2. CIRRUS INFRARED RADIATIVE TRANSFER

The observed upwelling radiance $I_{obs,N}$ in satellite channel "N" for an infinitesimally thin cirrus slab is expressed in terms of the cirrus bulk emissivity ϵ_{ci} as

$$I_{obs,N} = (1 - \epsilon_{ci,N}) I_{clr,N} + \epsilon_{ci,N} B_N(T_{ci}) t_{atm}, \quad (1)$$

where I_{clr} is the upwelling radiance for cirrus-free conditions, $B_N(T_{ci})$ is the Plank blackbody radiance for satellite sensor band N, and t_{atm} is the atmospehric transmittance between cirrus cloud top and the top of the atmosphere (TOA). Atmospheric transmittance is typically prescribed using radiative transfer codes and water-vapor/temperature soundings coincident with the satellite radiance observations. Conditions under which (1) must be used are discussed in later sections. The retrievals

described below make use of radiances from two window channels, M and N.

The quantities ϵ_{ci} and T_{ci} in Eq. (1) are descriptors of the spatial, radiative, and microphysical properties of a cirrus cloud. Exploiting a cloud mask (d'Entremont and Gustafson 2003) to identify nearby cirrus-free radiances provides an estimate for $I_{clr,N}$, leaving two unknowns in emissivity and effective temperature. With only one equation the solution is mathematically ill-posed; it is necessary to add at least one more equation to the problem. Writing Eq. (1) for two wavelength bands "N" and "M" yields

$$I_{obs,N} = (1 - \epsilon_{ci,N})\, I_{clr,N} + \epsilon_{ci,N}\, B_N(T_{ci}) , \qquad (2a)$$

$$I_{obs,M} = (1 - \epsilon_{ci,M})\, I_{clr,M} + \epsilon_{ci,M}\, B_M(T_{ci}) , \qquad (2b)$$

which at the outset appears to be a well-posed set of two equations in two unknowns ϵ_{ci} and T_{ci}. However the cirrus emissivity $\epsilon_{ci,N}$ is a wavelength-variant quantity with dependencies on the imaginary refractive index at wavelength λ_N, ice-particle size and shape, and the bimodality size distribution, SD. Thus in introducing a second equation we have also introduced a new unknown in $\epsilon_{ci,M}$. It is therefore necessary to relate $\epsilon_{ci,M}$ to the other "original" unknowns $\epsilon_{ci,N}$ and/or T_{ci}. To achieve this relation, a microphysics/radiation package is introduced that is comprised of climatological temperature-dependent information on ice particle shape and size distribution shape. This ice particle and SD shape information is explicitly coupled with a treatment for ice cloud optical properties known as the modified anomalous diffraction approximation (MADA; Mitchell et al. 1996; Mitchell 2000; Mitchell 2002; Mitchell et al. 2006). Using this model, the emissivity for any wavelength can be retrieved (and closure obtained) once an initial ϵ_{ci} and T_{ci} are retrieved. This package of ice cloud microphysical and radiative properties will now be described.

2.1 Ice cloud microphysical and radiative properties

Ice cloud emissivities and their associated absorption optical depths (τ_{abs}) depend on ice crystal shape (Mitchell and Arnott 1994), mean or effective ice particle size, and the SD shape or bimodality (Mitchell 2002). At this time we have not found a way to retrieve all these properties using thermal wavelengths, since the microphysical information

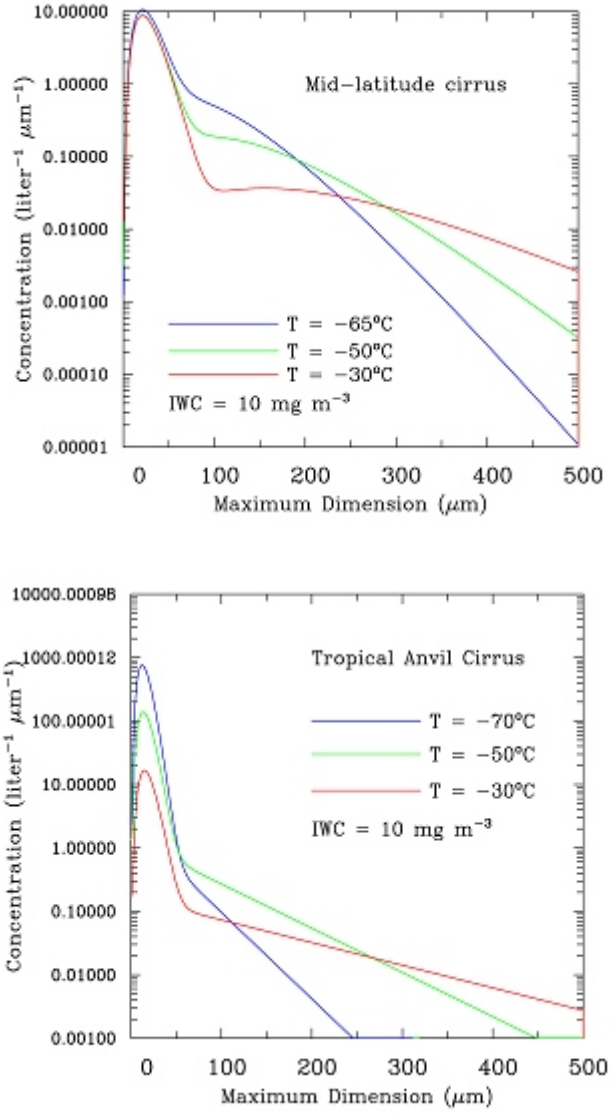

Figure 1. Examples of SDs from the mid-latitude and tropical anvil cirrus schemes, which are diagnosed as a function of temperature and ice water content (IWC).

content of window-region radiance observations is limited. On the other hand, thermal retrievals have an advantage in that the phase function or asymmetry parameter "g" is fairly well characterized due to strong forward scattering, and infrared cloud emissivities are generally not sensitive to the phase function or g. This reduces uncertainties relative to retrievals using solar channels. Therefore, to obtain closure in our retrievals, we introduce *a priori* information on ice particle and size distribution shapes.

Parameterizations using temperature and ice water content (IWC) as inputs have been developed for diagnosing the SD for (1) mid-latitude cirrus clouds (Ivanova et al. 2001) and (2) tropical anvil cirrus clouds (Ivanova 2004). The SDs are bimodal in each case, with each mode represented by a gamma distribution of the form

$$N(D) = N_o D^{\nu} \exp(-\Lambda D) . \quad (3)$$

These SDs are illustrated in Fig. 1 as a function of temperature. In the tropical SD scheme, the small mode increases with decreasing temperature, whereas the opposite occurs in the mid-latitude scheme. This results in very different cirrus radiative properties between these schemes for a given IWC. The mean ice particle size and the SD bimodality (i.e. ν and Λ for each mode) are determined solely from temperature, and temperature can be retrieved via the Plank function in (2). This leaves particle shape as the remaining unspecified property required for closure.

The percentages of ice particle shapes in ice clouds are being characterized climatologically with the advent of the Cloud Particle Imager (e.g. Lawson et al. 2001). The percentages of various ice crystal shapes are given at three different temperatures in Lawson et al. (2006) for mid-latitude cirrus clouds for maximum dimension D > 50 μm. Based on this information, the temperature-dependent crystal shape recipe described in Fig. 2 was developed, which is appropriate for the large mode. At temperatures between -25 and -55 °C, the recipe is representative of 22 Learjet flights in over 15,000 km of mid-latitude cirrus. Crystal shape percentages outside this range constitute educated guesses based partially on observed trends in the data. The crystal shape recipe for tropical cirrus assumes 30% columns, 5% plates and 65% planar polycrystals in the large mode of the SD, based on observations of ice crystal shape in tropical anvil cirrus reported in the literature (e.g. Heymsfield et al. 2002; Connelly et al. 2004, Garrett et al. 2005). Crystal shape percentages for the small mode for mid-latitude and tropical anvil cirrus are shown in Table 1. These percentages for tropical anvils are based on 13 DC-8 flights and about 100,000 particles near the tops of anvils in the tropical western Pacific, near Kwajalein atoll in the Marshall Islands. The mid-latitude percentages were estimated from random inspection of CPI images (Paul Lawson, personal communication).

The MADA scheme for radiative properties is formulated in terms of ice particle projected area- and mass-dimension power law relationships, which are unique for each ice particle shape. It is also formulated in terms of the six gamma SD parameters of a bimodal SD (i.e. one set of parameters per mode; see Eq. 3). It is thus explicitly coupled with the *a priori* information described above. The MADA has been formulated to treat any ice particle shape recipe.

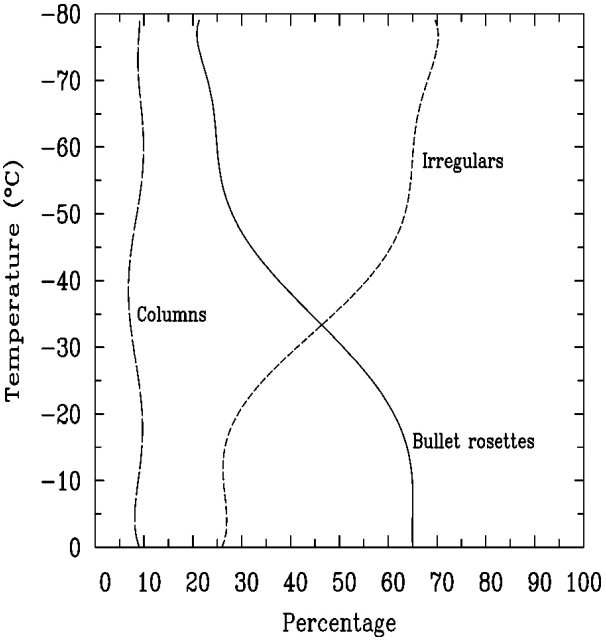

Figure 1. Temperature-dependent crystal shape recipe for the large mode of the SD for mid-latitude cirrus clouds.

2.2 Ice Particle Area- and Mass-Dimensional Power Laws

The retrieval of IWP and D_{eff} are sensitive to the ice particle shape assumed, which is the same as saying they are sensitive to the projected area- and mass-dimensional (P-D and m-D) power law relationships that represent various ice particle shapes in MADA. The constants used here in the P-D and m-D relations are listed in Table 2, along with references. Unfortunately the m-D power law for "irregular" ice crystals has not been characterized, so we have had to assume a relationship based on 2-dimensional images from the Cloud Particle Imager (CPI; see Lawson et al. 2001). Irregular crystals, as shown in Lawson et al. (2006), appear to be blocky or brick-like in shape, with a relatively large amount of mass per unit length. Their m-D power law for D > 100 μm is based on the

assumption that an irregular crystal has the same mass as a hexagonal column when D = 50 μm and has 2.5 times the mass of a bullet rosette at 300 μm. Note that the mass of a short (low-aspect ratio) hexagonal column at 300 μm is 4 times the mass of a bullet rosette at this size.

The m-D expression for D < 100 μm can be estimated if one is having some confidence on the P-D relationship. The P-D relation for compact polycrystals (Mitchell et al. 1996) agrees with the P-D power law for irregular crystals (Lawson et al. 2006; valid for D > 50 μm) within 10% for 150 μm < D < 500 μm. For D < 100 μm, the Lawson formula yields areas approaching that of a sphere, whereas the compact polycrystal expression yields areas similar to that of a square for a given D. Therefore the P-D power law for compact polycrystals was used to represent irregular ice particles at all sizes.

With reasonable confidence in the P-D relationship, one can estimate the m-D power law for D < 100 μm by determining the linear relation between the effective photon path d_e (i.e. the ratio P/ρ_i m, where ρ_i = density of bulk ice) and D as described in Mitchell and Arnott (1994). This d_e-D relationship can be determined by noting d_e is zero when D = 0, and evaluating another d_e-D pair near D = 100 μm where one has reasonable confidence in P and m. The resulting relation $d_e = \gamma D$ gives mass as $m = \gamma \rho_i \sigma D^{\delta+1}$, where $P = \sigma D^{\delta}$. This mass relation for 0 < D < 100 μm can be used to generate the constants α and β in the m-D relation $m = \alpha D^{\beta}$, which are given in Table 2.

3. RETRIEVAL OF ICE WATER PATH

The retrieval of IWP or liquid water path (LWP) makes use of the emissivity ϵ retrieved from any thermal wavelength in an atmospheric "window" (i.e. where absorption by atmospheric gases is minimal). The derivation of the equation that relates IWP to ϵ when scattering is negligible is given in Appendix A. Regarding IWP, if T_{ci} can be retrieved, then the SD parameters that determine D_{eff} (ν and Λ for each mode) can be diagnosed, and based on these SD parameters, the MADA gives the SD area weighted absorption efficiency $\overline{Q}_{abs}$ for any given wavelength. Note that

$$\overline{Q}_{abs} = \beta_{abs} / P_t , \qquad (4)$$

where β_{abs} is the absorption coefficient of the SD and P_t is SD projected area. This information can now be used to determine IWP at any given "window" wavelength λ:

$$IWP = \frac{2 \rho_i D_{eff} \ln(1 - \epsilon) \cos\theta}{3 \overline{Q}_{abs}} , \qquad (5)$$

where θ is the instrument viewing angle (cos θ = 1 at zenith) and ρ_i is the bulk density of ice (0.917 g cm^{-3}). IWPs at each λ can be averaged (provided ϵ(λ) is unsaturated) to produce a mean IWP, and an estimate of precision is obtained from the standard deviation.

Mathematically, closure can be demonstrated by equating the rhs of (5) at two different wavelengths (M and N), noting that ϵ and $\overline{Q}_{abs}$ are functions of λ. This yields the expression

$$\epsilon_M = 1 - [1 - \epsilon_N]^{(\overline{Q}_{abs,M} / \overline{Q}_{abs,N})} \qquad (6)$$

Since $\overline{Q}_{abs,M}$ and $\overline{Q}_{abs,N}$ are only functions of the SD (i.e. Λ and ν) and λ, and the SD is a function of temperature, then by knowing the two satellite sensor wavelengths, ϵ_N and T_{ci}, ϵ_M can be determined.

The relationship between cloud emissivity and IWP and its complex dependence on ice particle size and shape is illustrated in Fig. 3 and 4. The curves were generated using MADA, the SD scheme for mid-latitude cirrus (Ivanova et al. 2001) and the indicated ice crystal shape information. Scattering was accounted for, and cloud emissivities were calculated as

$$\epsilon = 1 - T - R \qquad (7)$$

where T = transmissivity and R = reflectivity for a given λ. This requires knowledge of the asymmetry parameter "g"at thermal wavelengths, which is not treated by MADA. We use the parameterization of Yang et al. (2005) to determine g for cirrus clouds as a function of D_{eff}. A two-stream model provided by Dr. John Edwards from the Hadley Centre for Climate Prediction and Research, U.K. Meteorological Office, was used with MADA to create these figures. This two-stream model, which includes scattering effects, is used in the Unified Model (i.e. the Hadley Centre GCM) for terrestrial radiation. One may also employ more sophisticated radiation transfer models using this retrieval methodology.

Figures 3 and 4 show the IWP range over which the IWP retrievals are valid for wavelengths at 8.55 μm and 3.74 μm, respectively. Both wavelengths correspond to VIIRS imager bands to be flown on upcoming NPOESS satellites. These figures illustrate the importance of having *a priori*

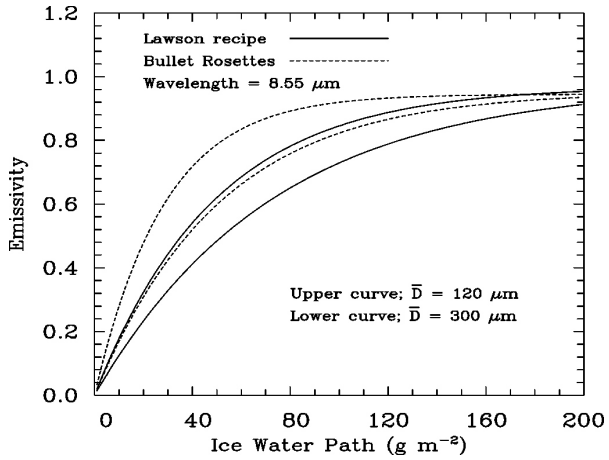

Figure 3. IWP-ϵ relationships for the mid-latitude cirrus crystal shape recipe and bullet rosettes. Each pair of curves represents ± 1 standard deviation from the average measured $\overline{D}$, showing the uncertainty in IWP when $\overline{D}$ is not known.

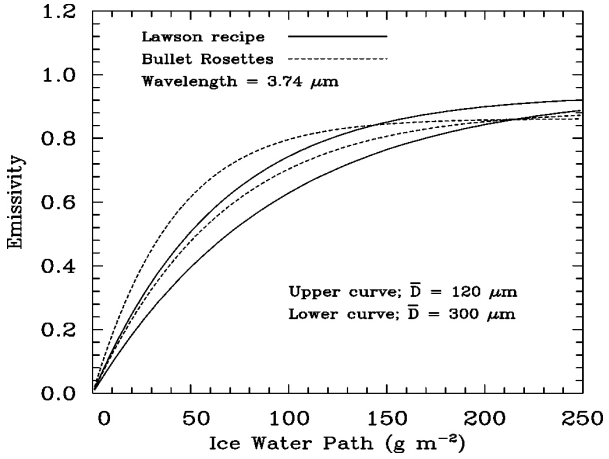

Figure 4. Same as Fig. 3 except for the wavelength band centered at 3.74 μm.

information on ice particle shape as part of one's retrieval scheme. If the ice particle shape composition is approximately known, then natural variability in ice particle size (i.e. $\overline{D}$) does not introduce excessive uncertainty in the IWP retrieval. In the study by Ivanova et al. (2001), about 1000 SDs were evaluated from various cirrus field campaigns. The mean size of the large mode of the SD, $\overline{D}$, was 210 μm ± 90 μm. Figures 3 and 4 show the emissivity-IWP relationship for one standard deviation from $\overline{D}$ for the Lawson recipe and for bullet rosettes, a common ice crystal habit in cirrus clouds. The Lawson recipe accounts for irregular shaped ice crystals that may be overlooked in qualitative appraisals of ice crystal shape economies. For the Lawson shape recipe, the uncertainty in IWP is about ± 20% or less for λ = 8.55 μm and about ± 17% or less for λ = 3.74 μm. Obviously in the absence of ice particle shape information, uncertainties are much greater. The reduced uncertainty associated with the 3.74 μm channel is due to weaker absorption (more mass-dependent absorption) at this wavelength. If D_{eff} was also retrieved, this might reduce IWP uncertainties. Such retrievals are discussed in the next section.

The main reason the ϵ-IWP curves for bullet rosettes are different than those for the Lawson recipe is that the relatively massive irregular crystals contribute substantially to the Lawson recipe. For a given IWP consisting of only irregular crystals, there will be fewer irregular crystals than if only bullet rosettes existed, and the projected area associated with irregular crystals will be relatively low. This results in decreased emissivities for irregular crystals for a given IWP.

For the 3.74 μm channel, IWP values at least up to 250 g m^{-2} can be retrieved (Fig. 4), while for the 8.55 μm channel, values up to about 200 g m^{-2} can be retrieved (Fig. 3). At 3.74 μm, the curves begin to asymptote at lower ϵ relative to 8.55 μm. This is due to mass-dependent absorption and greater scattering by ice particles at 3.74 μm. One disadvantage of using the 3.74 μm channel is that during the daytime, both the terrestrial and solar radiation spectrum contribute to the radiances.

4. RETRIEVAL OF EFFECTIVE DIAMETER IN CIRRUS CLOUDS

As described in Mitchell (2002), effective diameter can be universally defined for both liquid water and ice clouds as

$$D_{eff} = \frac{3\ WC}{2\ \rho\ P_t} \qquad (8)$$

where WC is the water content (units = g m^{-3}), ρ is the bulk density of water or ice (units = g cm^{-3}) and P_t is the projected area of the size distribution SD (units = cm^2 m^{-3}). At thermal wavelengths, radiance information on ice particle size results from its dependence on the absorption efficiency, Q_{abs}. We thus use ratios of $\overline{Q}_{abs}$ at two wavelengths to estimate D_{eff}. In practice, the absorption optical depth, τ_{abs}, is retrieved since ratios of τ_{abs} at two

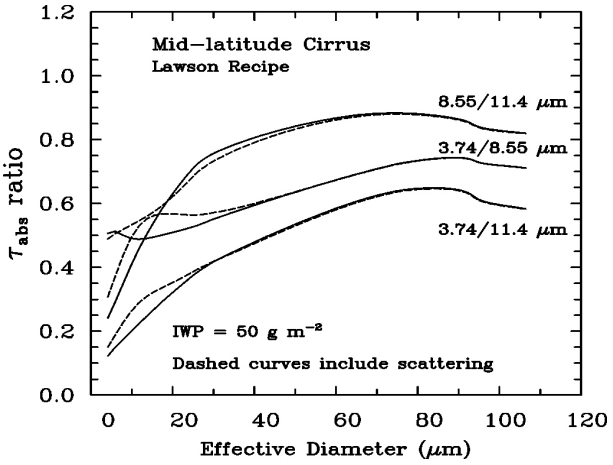

Figure 5. Possible relationships for retrieving D_{eff} in mid-latitude cirrus clouds.

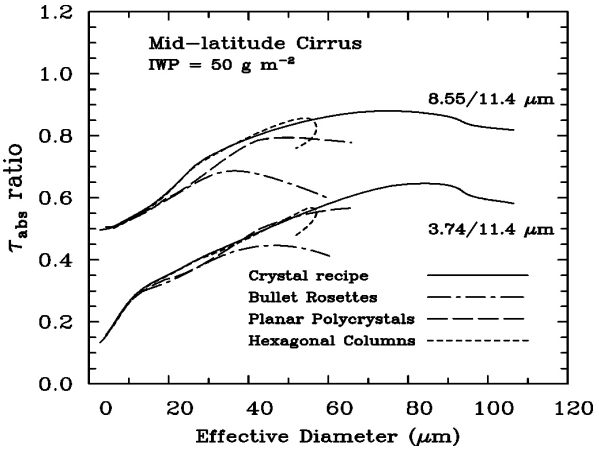

Figure 6. Sensitivity of D_{eff} retrievals to ice crystal shape in mid-latitude cirrus clouds. All curves include scattering effects.

wavelengths are equivalent to ratios of $\overline{Q}_{abs}$. That is, the SD (i.e. P_t) dependence of τ_{abs} cancels when taking ratios, yielding the $\overline{Q}_{abs}$ ratio. Effective thermal window wavelength combinations or ratios for retrieving D_{eff} consist of (1) τ_{abs} for relatively weak absorption in the wavelength range 3.7- 4.0 μm divided by τ_{abs} for strong absorption (i.e. 10.8 - 12.5 μm); (2) τ_{abs} for moderate absorption (8.3 - 10.0 μm) divided by τ_{abs} for strong absorption; and (3) τ_{abs} for relatively weak absorption divided by τ_{abs} for moderate absorption. To calculate τ_{abs}, its relation to the cloud transmissivity T is inverted:

$$\tau_{abs} = -\ln T \, . \qquad (9)$$

But since T is not retrieved, we estimate τ_{abs} by ignoring scattering, using only ϵ:

$$\tau_{abs} = -\ln(1 - \epsilon). \qquad (10)$$

4.1 Mid-latitude cirrus clouds

To determine whether cirrus clouds contain radiance information from which D_{eff} could be retrieved, the MADA scheme was used to relate τ_{abs} ratios to D_{eff} using the ratio combinations described above. This is shown for mid-latitude cirrus clouds in Fig. 5 for the Lawson crystal shape recipe, where the solid curves correspond to the zero-scattering assumption. This assumption appears to be generally good. As noted, the Lawson crystal shape recipe contains a substantial percentage of "irregular"crystals (shown in Fig. 4 of Lawson et al. 2006) that appear to have relatively large masses for a given maximum dimension D. These relatively massive crystals are responsible for the crystal-recipe curves in Fig. 5 extending to relatively large values of D_{eff}. In fact, some D_{eff} retrievals may be underestimating D_{eff} due to the neglect of these massive ice crystals in the SD algorithm assumptions.

None of the τ_{abs} ratio combinations in Fig. 5 yield a τ_{abs}-D_{eff} curve that provides a unique value for D_{eff} at every corresponding value of τ_{abs}. We thus tentatively conclude that a comprehensive method for retrieving any value of D_{eff} at terrestrial wavelengths is very much in question for mid-latitude cirrus clouds, even when scattering is accounted for. This is because τ_{abs} ratios are really ratios of $\overline{Q}_{abs}$, and $\overline{Q}_{abs}$ is the only radiative property at thermal wavelengths that is likely to be exploited for size information. Nonetheless, D_{eff} can still be approximated as a function of temperature. Since T_{ci} is retrieved, the SD scheme of Ivanova et al. (2001) can be used to approximate D_{eff} and reduce uncertainties in the retrieval of IWP in mid-latitude cirrus clouds.

The reason unique solutions for D_{eff} are not obtained for mid-latitude cirrus clouds is because of the relationship between the small and large modes of the SD. As the large mode broadens, the amplitude of the small mode increases, so much so that $\overline{Q}_{abs}$ decreases slightly. This creates a situation where the same τ_{abs} ratio may correspond to two D_{eff} values.

The sensitivity of the D_{eff} retrievals to ice crystal shape is shown in Fig. 6 for mid-latitude cirrus clouds. This illustrates how the τ_{abs} ratios

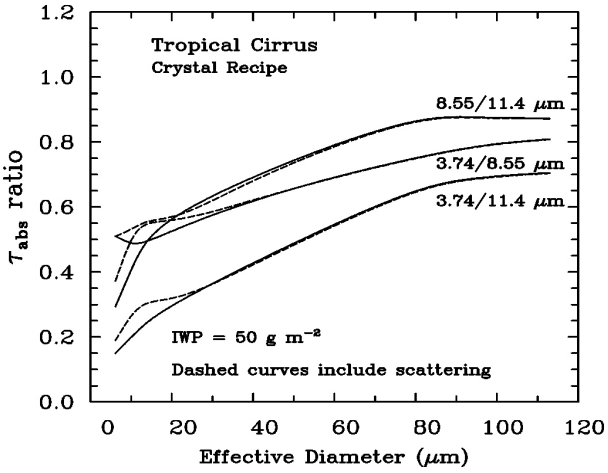

Figure 7. Possible relationships for retrieving D_{eff} in tropical anvil cirrus clouds.

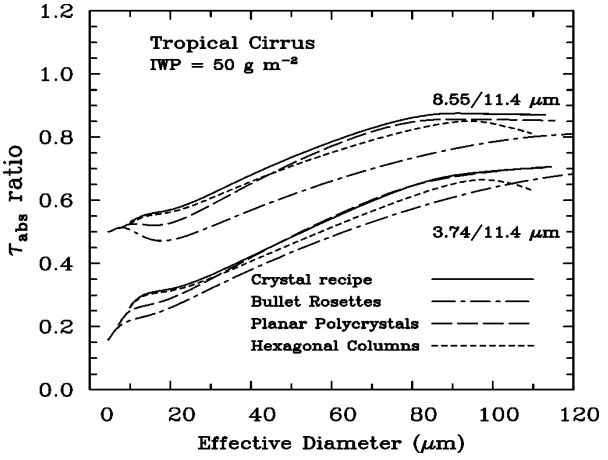

Figure 8. Sensitivity of D_{eff} retrievals to ice crystal shape in tropical anvil cirrus clouds.

depend on ice crystal shape and underscores the need for *a priori* information on ice particle shape in retrieval algorithms.

4.2 Tropical anvil cirrus clouds

Because the relationship between the small and large modes of the SD for tropical anvil cirrus is opposite that of mid-latitude cirrus, the τ_{abs} ratio yields unique solutions for D_{eff} in this case, as shown in Fig. 7. The τ_{abs} ratio based on 3.74 and 8.55 μm appears best suited for retrieving D_{eff}, although using the 3.74 μm channel may require nighttime conditions. The sensitivity of the D_{eff} retrieval to ice particle shape is shown in Fig. 8. If bullet rosettes turn out to be a minor constituent in anvil cirrus, as some studies suggest (Baran et al. 1998; Connolly et al. 2004), then the crystal shape dependence of tropical anvil D_{eff} retrievals will be considerably less.

5. LIQUID WATER CLOUDS

In the case of liquid water clouds, the situation is simplified in some ways since (1) the cloud droplets all have the same shape, reducing retrieval uncertainties and (2) the SD is generally monomodal, allowing D_{eff} to be retrieved. On the other hand, ϵ can be more sensitive to radiation scattering. The procedure for retrieving the LWP is similar to that for obtaining IWP in cirrus clouds: first retrieve D_{eff} from the τ_{abs} ratio, and second retrieve LWP from the emissivity. The radiative properties are calculated from Mie theory, and the Hadley Centre two-stream model noted above can be used to treat scattering. Cloud droplet size spectra were represented as monomodal using (3) with v = 10. The retrieval method should work well with passive ground-based infrared interferometers, such as the Atmospheric Emitted Radiance Interferometer, (AERI (Knuteson et al. 2004)). AERI radiances can be used to retrieve emissivities at many wavelengths in the atmospheric window regions provided coincident lidar and/or radar, and sonde temperature-profile measurements are available, as described in DeSlover et al. (1999).

5.1 Effective Diameter

The at 8.55/11.4 μm τ_{abs} ratio and the 3.74/11.4 μm τ_{abs} ratio are shown as a function of D_{eff} in Fig. 9, where τ_{abs} is given by (10). The zero-scattering relationship is shown by the dashed curves. When the LWP is less than 50 g m^{-2}, the 3.74/11.4 μm τ_{abs} ratio-D_{eff} relationship is insensitive to scattering by water droplets. Both τ_{abs} ratio-D_{eff} relationships yield unique D_{eff} values for any given τ_{abs} ratio over the expected range of D_{eff} as LWP is incremented up to 100 g m^{-2} or higher. Thus either or both relationships can be used to retrieve D_{eff} as outlined in Section 5.4.

5.2 Liquid Water Path

The relationship between LWP and emissivity ϵ is shown in Fig 10 for λ = 3.74 μm. The weaker absorption at this wavelength provides a greater range for LWP retrievals. When LWP < 30 g m^{-2}, a somewhat unique relationship exists

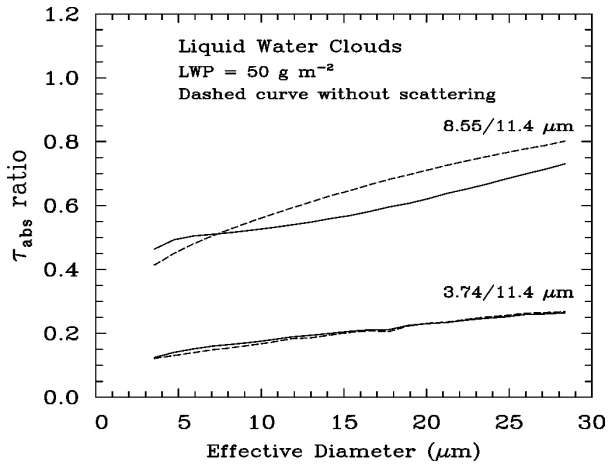

Figure 9. Relationships for retrieving D_{eff} in liquid water clouds.

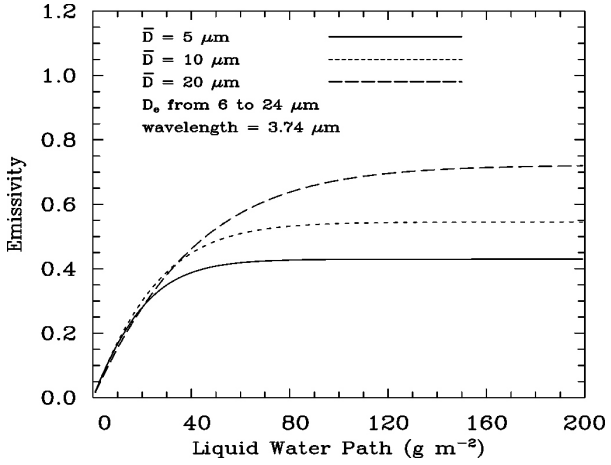

Figure 10. Dependence of ϵ on $\overline{D}$ and LWP, used for the retrieval of LWP.

between ϵ and LWP. At higher LWP, scattering becomes important and the ϵ-LWP relationship becomes strongly dependent on D_{eff}. This is illustrated in Fig. 10, where the modeled curves correspond to $\overline{D}$ (or D_{eff}) over their normal range of natural variability. It is seen that for $\overline{D}$ = 5 μm, the limit for retrieving LWP is about 60 g m^{-2}. For $\overline{D}$ = 10 μm, the limit is about 80 g m^{-2}, and for $\overline{D}$ = 20 μm, the limit is about 120 g m^{-2}. Thus, under most conditions, the LWP retrieval range may be about 5 to 80 g m^{-2} or better. This method should complement the MWR LWP retrievals fairly well, which have an uncertainty of about 30% when LWP = 80 g m^{-2}, with less uncertainty at higher LWPs.

It was found that by varying the value of the dispersion parameter ν in (3) between 5 and 13 that the uncertainty in LWP was only ± 4%.

5.3 Optical Depth

Finally, visible optical depth τ is estimated from the retrieved LWP and D_{eff}:

$$\tau = 3\,LWP / (\rho_w D_{eff}) \qquad (11)$$

which is based on the assumption that at visible wavelengths, extinction efficiency $Q_{ext} = 2$. Note that (11) is also used to calculate τ for cirrus clouds.

5.4 Retrieval Method

Many approaches may be used that minimize computational time and expense, but in principle, one begins with retrievals of cloud emissivity at two or three different wavelengths as described above. Emissivities are inverted using (10) to yield a τ_{abs} ratio. Then the radiation algorithm is run with an initial LWP value, and adjusting $\overline{D}$ until the theoretically predicted and observed values of the τ_{abs} ratio match. Then the measured ϵ at 3.74 μm is compared with the predicted ϵ at 3.74 μm. If convergence is not met, the LWP is incremented and the cycle is repeated until both the predicted and measured τ_{abs} ratios and ϵ at 3.74 μm match or meet the convergence criteria. This yields the LWP. Finally, using the LWP and D_{eff}, the visible optical depth is retrieved via (11). This general methodology may also be successfully applied to remote sensing from satellites to obtain D_{eff}, LWP and τ, as well as the passive ground-based and space-based remote sensing of cirrus clouds to obtain D_{eff}, IWP and τ.

6. PHASE DISCRIMINATION

It may be possible to discriminate the phase of the cloud (liquid water or ice) by using the τ_{abs} ratio at 3.74/11.4 μm. As shown in Figs. 5-8 and 9, this ratio is generally greater than 0.25 for ice clouds and is generally less than 0.25 for liquid water clouds. This occurs since (1) the imaginary index of refraction for bulk ice is about twice as large as the corresponding value for liquid water at 3.74 μm, and (2) ice crystals tend to be larger than water droplets. Both factors contribute to larger $\overline{Q}_{abs}$ values for ice clouds, providing a convenient means of phase discrimination.

7. RESULTS

To demonstrate the performance of this methodology for mid-latitude cirrus clouds, the ground-based AERI instrument was used to retrieve D_{eff}, IWP and τ for the 9 March 2000 cirrus case study at the Southern Great Plains (SGP) ARM site, as shown in Fig. 11. Since the retrieval was for mid-latitude cirrus, unique solutions for D_{eff} are only possible below a certain τ_{abs} ratio. For AERI observation times greater than 21.2 UTC, non-unique D_{eff} solutions occur and D_{eff} values, though larger than about 65 μm, are highly uncertain. But since only larger D_{eff} values are non-unique, the percent uncertainty should generally not be greater than about 40%.

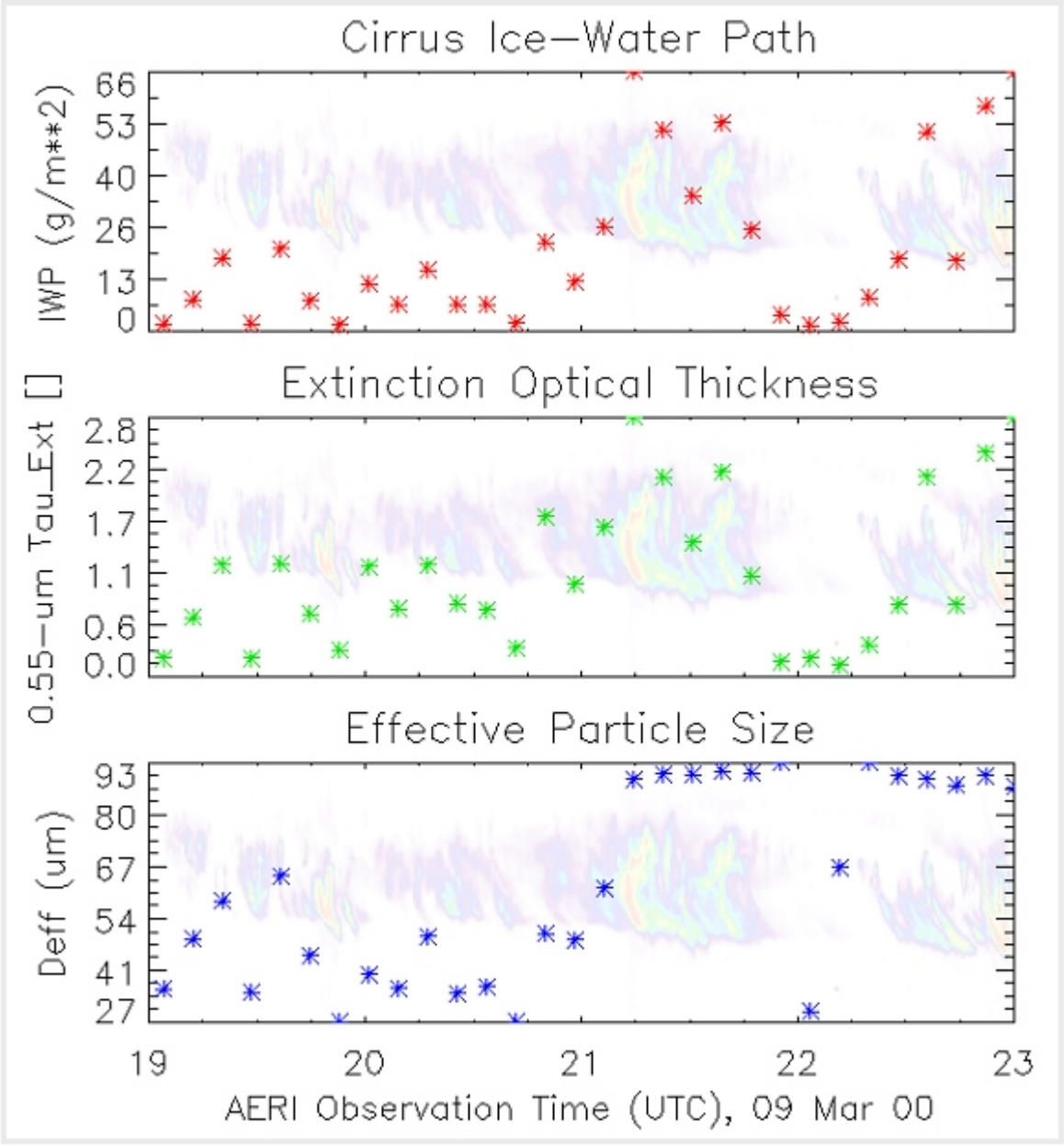

Figure 11. Example of mid-latitude cirrus retrievals using the 9 March 2000 case study during a DOE-ARM IOP (Intensive Observation Period). The time-series of radar reflectivities of the cirrus are superimposed on each panel to aid in interpreting the retrievals.

Retrievals of IWP in mid-latitude cirrus corresponding to non-unique D_{eff} retrievals should have less uncertainty than the D_{eff} retrievals. This is because $\overline{Q}_{abs}$ is a function of D_{eff} (see Eq. A5), and Eq. 5 tells us that the dependence of IWP on D_{eff} will not be linear (i.e. proportional to D_{eff}), but will be weaker than this. The "D_{eff} cancellation" effect in (5) will be greater for weaker absorption (e.g. λ = 3.74 μm) since the dependence of $\overline{Q}_{abs}$ on D_{eff} becomes more linear as absorption becomes more mass-dependent.

The cirrus case study evaluated in Fig. 11 was also used in a ground-based retrieval intercomparison study (Comstock et al. 2006). An earlier version of our cirrus cloud property retrieval method was compared against 11 other active and passive methods for retrieving visible optical depth (OD) and IWP. Several other methods yielded ODs and IWPs similar to our own values.

8. SUMMARY AND CONCLUSIONS

A methodology has been described for retrieving D_{eff}, WP (IWP or LWP) and τ from satellite sensors or passive ground-based infrared radiometers. This applies to both liquid water and ice clouds, and a means of discriminating water phase is described. For cirrus clouds, the retrieval of these properties depends considerably on the bimodality of the size distribution (i.e. the relationship between the small and larger ice particle modes). A given τ_{abs} ratio may correspond to a considerably different D_{eff} value for a mid-latitude cirrus cloud than for a tropical anvil cirrus cloud. In addition, D_{eff} retrievals using infrared radiances should depend substantially on ice particle shape. These findings underscore the importance of incorporating climatologies of ice particle and size distribution shape appropriate to mid-latitude and tropical anvil cirrus in cloud property retrieval schemes.

The retrieval range for IWP is about 5-250 g m^{-2}, which appears to coincide with the range of IWP observed in most cirrus clouds. The retrieval range for LWP under most conditions is about 5 to 80 g m^{-2} or better. This fills an important gap, since this is precisely the range over which LWP retrievals from the microwave radiometer (MWR) perform poorly.

Uncertainties associated with the water cloud retrievals appear to be on the order of ± 5% based on theoretical calculations, but this scheme has only recently been developed and much testing is still needed. The main factors contributing to the uncertainty in cirrus cloud retrievals, namely particle shape and size distribution shape, are not an issue for liquid water clouds. Regarding cirrus clouds, if the percentages of various ice particle shapes can be reasonably approximated from *a priori* particle shape information for each mode of the size distribution, then the uncertainty in IWP retrievals should be no worse than ± 20%. This uncertainty should be considerably less for tropical anvil cirrus, where D_{eff} can be retrieved with better accuracy.

AKNOWLEDGMENT

This work was funded by the U.S. Department of Energy, Environmental Sciences Division, Atmospheric Radiation and Measurement (ARM) Program, which is gratefully thanked for its support. We extend our thanks to Dr. John Edwards at the Hadley Centre for providing the two-stream model used for treating scattering in the infrared.

Table 1. Ice crystal shape recipes in percent by number concentration for the small crystal mode of mid-latitude and tropical anvil cirrus clouds.

Crystal shape	Mid-latitude cirrus	Tropical anvil cirrus
Quasi-spherical	53	44.6
irregular	31	48.4
bullet rosette	16	0
hexagonal columns	0	5.6
hexagonal plates	0	1.4

Table 2. Projected area- and mass-dimensional power law constants for relationships of the form $P = \sigma D^{\delta}$ and $m = \alpha D^{\beta}$ that were used in MADA.

Crystal shape	small mode of SD				large mode of SD			
	σ	δ	α	β	σ	δ	α	β
quasi-spherical[1]	0.5414	2.000	0.21875	3.000	0.5414	2.000	0.21875	3.000
irregular[2]	0.4715	2.000	0.20935	3.000	0.4715	2.000	0.06150	2.734
planar polycrystals[3]	0.2285	1.880	0.0581	2.879	0.2285	1.880	0.007389	2.449
bullet rosette[4]	0.1470	1.750	0.0260	2.750	0.1404	1.740	0.0260	2.750
hexagonal columns[5]	0.6837	2.000	0.2515	3.000	0.0459	1.415	0.001658	1.910
hexagonal plates[6]	0.2395	1.855	0.04953	2.852	0.2395	1.855	0.007389	2.449

1: Nousian and McFarquhar, 2005
2: Lawson et al. 2006 (area); see text for mass
3: Mitchell et al. 1996
4: Lawson et al., 2006 (area); Heymsfield et al., 2002 (mass)
5. Mitchell et al., 1996; Mitchell and Arnott, 1994 (large mode mass)
6. Auer and Veal, 1970 (area); Mitchell and Arnott, 1994; Mitchell et al., 1996 (mass)

APPENDIX A: Dependence of IWP on Emissivity

The following is a derivation of the relationship between IWP, emissivity ϵ, effective diameter D_{eff}, and satellite viewing angle θ. If we assume no scattering at thermal wavelengths:

$$\epsilon = 1 - \exp(-\tau_{abs}/\cos\theta) , \quad (A1)$$

where τ_{abs} is the absorption optical depth. For a cirrus cloud where the SD is invariant with in-cloud position,

$$\tau_{abs} = \beta_{abs} \Delta z , \quad (A2)$$

where Δz = cloud physical depth and β_{abs} is the absorption coefficient, defined as:

$$\beta_{abs} = \int Q_{abs}(D, \lambda) P(D) N(D) dD , \quad (A3)$$

where Q_{abs} is the absorption coefficient, P is the projected area of an ice particle of maximum dimension D, N(D) is the size distribution and λ is the wavelength. The dependence of Q_{abs} on λ is very complex but is predicted by MADA theory. However, in situ measurements and theoretical work (Baran et al. 2003; Mitchell et al. 2006) indicate that the photon tunneling process may contribute relatively little to absorption for ice crystals having complex shapes. For such conditions, Q_{abs} may be well approximated (Mitchell 2002) by the anomalous diffraction approximation (ADA) as given in Mitchell and Arnott (1994):

$$Q_{abs,ADA} = 1 - \exp(-4 \pi n_i d_e / \lambda) , \quad (A4)$$

where n_i is the imaginaray index of refraction and d_e = effective photon path for a single ice particle. Note $d_e = V/P$, where V = volume at bulk ice density ρ_i. Since D_{eff} is simply d_e but for the entire size distribution, we may substitute D_{eff} for d_e in (A4), but noting that the diameter of a sphere is 3/2 d_e :

$$\overline{Q}_{abs,ADA} = 1 - \exp(-8 \pi n_i D_{eff} / 3 \lambda) , \quad (A5)$$

where $\overline{Q}_{abs,ADA}$ represents Q_{abs} for the entire SD. This allows Q_{abs} to go outside the integral in (A3) as $\overline{Q}_{abs}$ (Mitchell 2002), making the integral the total projected SD area, P_t . Hence, (A3) can be formulated as

$$\beta_{abs} = \overline{Q}_{abs,ADA} P_t , \quad (A6)$$

and τ_{abs} is expressed as

$$\tau_{abs} = \overline{Q}_{abs,ADA} P_t \Delta z . \quad (A7)$$

Calculations of τ_{abs} and ϵ using (A7) yield essentially identical values as determined using the scheme of Mitchell (2002), which uses an exact solution of (A3). Equation (A7) can now be combined with (1) to solve for IWP, noting that (1) can be written as

$$D_{eff} = 3 IWP /(2 \rho_i P_t \Delta z) , \quad (A8)$$

giving

$$IWP = 2 \rho_i D_{eff} \tau_{abs} /(3 \overline{Q}_{abs,ADA}). \quad (A9)$$

Substituting for τ_{abs} in (A1) using (A9), (A1) can be rewritten as

$$\epsilon = 1 - \exp(-3 IWP \overline{Q}_{abs,ADA} / 2 \rho_i D_{eff} \cos\theta) . \quad (A10)$$

Inverting (A10) to solve for IWP,

$$IWP = \frac{-2 \rho_i D_{eff} \ln(1 - \epsilon) \cos\theta}{3 \overline{Q}_{abs,ADA}} . \quad (A11)$$

Knowing the wavelength and the retrieved D_{eff} provides $\overline{Q}_{abs,ADA}$ via (A5), and IWP is readily solved for. In practice, the modified anomalous diffraction approximation (MADA) is used instead of (A5) to calculate $\overline{Q}_{abs}$ (Mitchell 2002) so that tunneling and internal reflection/refraction contributions to absorption are considered, as well as SD bimodality.

REFERENCES

Baran, A.J., J.S. Foot and D.L. Mitchell, 1998: Ice-crystal absorption: a comparison between theory and implications for remote sensing. *Appl. Opt.*, **37**, 2207-2215.

Comstock, J.M., R. d'Entremont, D. DeSlover, G.G. Mace, S.Y. Matrosov, S.A. McFarlane, P. Minnis, D. Mitchell, K. Sassen, M.D. Shupe, D.D. Turner, and Zhien Wang, 2006: An intercomparison of microphysical retrieval algorithms for upper tropospheric ice clouds. Submitted to the Bulletin of the American Meteorological Society.

Connolly, P.J., C.P.R. Saunders, W.M. Gallagher, K.N. Bower, M.J. Flynn, T.W. Choularton, J. Whiteway and R.P. Lawson, 2004: Aircraft observations of the influence of electric fields on the aggregation of ice crystals. *Q.J.R. Meteorol. Soc.*, **128**, 1-20.

d'Entremont, R.P., and G. Gustafson, 2003: Analysis of geostationary satellite imagery using a temporal-differencing technique. Earth interactions, 7, Paper 1.

DeSlover, D., W.L. Smith, P.K. Ppiironen and E.W> Eloranta, 1999: A methodology for measuring cirrus cloud visible-to-infrared spectral optical depth ratios. *J. Atmos. Ocean. Tech.*, **16**, 251-262.

Garrett, T.J., B.C. Navarro, C.H. Twohy, E.J. Jensen, D.G. Baumgardner, P.T., Bui, H. Gerber, R.L. Herman, A.J. Heymsfield, P. Lawson, P. Minnis, L. Nguyen, M. Poellot, S.K. Pope, F.P.J. Valero, and E.M. Weinstock, 2005: Evolution of a Florida Cirrus Anvil. *J. Atmos. Sci.*, **62**, 2352-2372.

Heymsfield, A.J., A. Bansemer, P.R. Field, S.L. Durden, J.L. Stith, J.E. Dye, W. Hall, and C.A. Grainger, 2002: Observations and parameterizations of particle size distributions in deep tropical cirrus and stratiform precipitating clouds: Results from in situ observations in TRMM field campaigns. *J. Atmos. Sci.*, **59**, 3457-3491.

Ivanova, D., D.L. Mitchell, W.P. Arnott and M. Poellot, 2001: A GCM parameterization for bimodal size spectra and ice mass removal rates in mid-latitude cirrus clouds. *Atmos. Res.*, **59**, 89-113.

Ivanova, D., 2004: Cirrus cloud parameterizations for global climate models (GCMs) and North American monsoon modeling study. Ph.D. dissertation, University of Nevada, Reno, 181 pp.

Lawson, R.P., B.A. Baker, C.G. Schmitt and T.L. Jensen, 2001: An overview of microphysical properties of Arctic clouds observed in May and July during FIRE-ACE. *J. Geophys. Res.*, **106**, 14,989-15,014.

Lawson, R.P., B. Baker, B. Pilson, and Q. Mo, 2006: In situ observations of the microphysical properties of wave, cirrus and anvil clouds. Part 2: Cirrus clouds. *J. Atmos. Sci.*, in press.

Mitchell, D.L., and W.P. Arnott, 1994: A model predicting the evolution of ice particle size spectra and radiative properties of cirrus clouds. Part II: Dependence of absorption and extinction on ice particle morphology. *J. Atmos. Sci.*, **51**, 817-832.

Mitchell, D.L., 1996: Use of mass- and area-dimensional power laws for determining precipitation particle terminal velocities. *J. Atmos. Sci.*, **53**, 1710-1723.

Mitchell, D.L., A. Macke, and Y. Liu, 1996: Modeling cirrus clouds. Part II: Treatment of radiative properties. *J. Atmos. Sci.*, **53**, 2967-2988.

Mitchell, D.L., 2000: Parameterization of the Mie extinction and absorption coefficients for water clouds. *J. Atmos. Sci.*, **57**, 1311-1326.

Mitchell, D.L., 2002: Effective diameter in radiation transfer: Definition, applications and limitations. *J. Atmos. Sci.*, **59**, 2330-2346.

Mitchell, D.L., A.J. Baran, W.P. Arnott and C. Schmitt, 2006: Testing and comparing the modified anomalous diffraction approximation. *J. Atmos. Sci.*, in press.

Knuteson,R.O., and co-authors, 2004: Atmospheric Emitted Radiance Interferometer (AERI). Part I: Instrument design. *J. Atmos. Oceanic Technol.*, **21**, 1763-1776.

Yang, P., H. Wei, H-L. Huang, B.A. Baum, Y.X. Hu, G.W. Kattawar, M.I. Mishchenko, and Q. Fu, 2005: Scattering and absorption property database for nonspherical ice particles in the near- through far-infrared spectral region. *Appl. Opt.*, **44**, 5512-5523.

Yoshida, Y., and S. Asano, 2005: Effects of the vertical profiles of cloud droplets and ice particles on the visible and near-infrared radiative properties of mixed-phase stratocumulus clouds. *J. Meteorol. Soc. Japan*, **83**, 471-480.